IOP PUBLISHING JOURNAL OF PHYSICS: CONDENSED MATTER
J. Phys.: Condens. Matter **24** (2012) 354001 (11pp) doi:10.1088/0953-8984/24/35/354001

Scattering of CO and N_2 molecules by a graphite surface

Junepyo Oh[1], Takahiro Kondo[1], Keitaro Arakawa[1], Yoshihiko Saito[1], Junji Nakamura[1], W W Hayes[2] and J R Manson[3]

[1] Graduate School of Pure and Applied Science, University of Tsukuba, 1-1-1 Tennoudai, Tsukuba, Ibaraki 305-8573, Japan
[2] Physical Sciences Department, Greenville Technical College, Greenville, SC 29606, USA
[3] Department of Physics and Astronomy, Clemson University, Clemson, SC 29634, USA

E-mail: Wayne.Hayes@gvltec.edu and jmanson@clemson.edu

Received 9 March 2012, in final form 22 May 2012
Published 16 August 2012
Online at stacks.iop.org/JPhysCM/24/354001

Abstract
Measurements of angular distributions for the scattering of well-defined incident beams of CO and N_2 molecules from a graphite surface are presented. The measurements were carried out over a range of graphite surface temperatures from 150 to 400 K and a range of incident translational energies from 275 to over 600 meV. The behavior of the widths, positions and relative intensities of the angular distributions for both CO and N_2 were found to be quite similar. The experimental measurements are discussed in comparison with calculations using a classical mechanical model that describes single collisions with a surface. Based on the behavior of the angular distributions as functions of temperature and incident translational energy, and the agreement between measured data and calculations of the single-collision model, it is concluded that the scattering process is predominantly a single collision with a collective surface for which the effective mass is significantly larger than that of a single carbon atom. This conclusion is consistent with that of earlier experiments for molecular beams of O_2 molecules and Xe atoms scattering from graphite. Further calculations are carried out with the theoretical molecular scattering model in order to predict translational and rotational energy transfers to and from the molecule during scattering events under similar initial conditions.

1. Introduction

Knowledge of the interactions of molecules with surfaces is important for understanding such fundamental processes as adsorption, desorption, energy transfer and heterogeneous chemical reactions. One method of gaining such knowledge is through scattering experiments in which well-defined beams of molecules are directed at a surface and the scattered products are subsequently detected [1, 2]. With this in mind the authors have embarked on an extensive study of the scattering of diatomic molecules from a graphite surface. The first of these was a study of the angular distributions for oxygen molecules scattered after a collision with a clean and ordered graphite surface [3, 4]. In this paper we present new data for the angular distributions of CO and N_2 molecules scattered from graphite.

The data presented here are for a large range of initial conditions, with incident beam energies ranging from 275 to 661 meV and surface temperatures from 150 to 400 K. The angular distributions have many of the characteristics of the earlier results for O_2. They are broad, single-peaked structures with a most probable intensity (peak position) at a slightly supraspecular angle. These characteristics are indicative of scattering mechanisms that are classical mechanical in nature, with large energy transfers involving the excitation of large numbers of phonon quanta.

These data are analyzed with a classical mechanical theory of molecule–surface scattering that has been shown previously to correctly predict the temperature and incident translational energy dependence for other systems [3–6]. Although both CO and N_2 are more massive than a single graphite carbon atom, the results of this analysis indicate that

the scattering is predominantly a single-collision event with a collective surface. The molecules scatter from a surface with an effective mass significantly larger than that of a single carbon atom implying that many carbon atoms are involved in the process. In previous molecular beam experiments on graphite, heavier projectiles such as O_2 and Kr have also been shown to make predominantly single-collision events with a collective surface [3, 7, 8]. In this case, the effective mass of the graphite surface for both CO and N_2 collisions is found to be approximately 1.8 rings of six-atom carbon (10.8 carbon atoms) which is the same value found previously for O_2/graphite scattering [3].

2. Experiment

We give only the essential parameters of the experimental system here, as the details of the molecule–surface scattering apparatus have been described elsewhere [9]. The molecular beam is created by free-jet expansion into vacuum from a gas of approximately 10% CO or N_2 seeded in He. The temperature of the nozzle and stagnation chamber is controlled to within a fluctuation of ± 0.1 K. The energy resolution of the incident beam translational energy E_i^T is given by a $\Delta E_i^T/E_i^T$ of less than 20%. The angular resolution is controlled by the skimmer and a downstream aperture and is less than 0.75°. The scattering chamber is maintained at an ultrahigh vacuum of better than 3×10^{-10} Torr. The detector is a quadrupole mass spectrometer at the end of an arm positioned perpendicularly to the incident beam which means that only those particles deflected through a total scattering angle of 90° enter the detector. Scattered particles are measured only in the scattering plane, i.e. the plane which contains the incident beam, the detector direction and the normal to the crystal sample surface. The crystal target is mounted so that it can be rotated through a polar angle with 0.1% accuracy. Thus with the incident and final polar scattering angles measured with respect to the normal to the surface, then $\theta_i + \theta_f = \pi/2$, implying that the angular intensity spectra reported here as functions of θ_f have a different incident angle θ_i for each θ_f.

The graphite crystal sample is highly oriented pyrolytic graphite, cleaved in air, then mounted on the sample holder and cleaned in high vacuum by heating to 800 K. The sample is cooled by a cryogenic refrigerator and heated by infrared radiation from a nearby hot tungsten filament with the temperature controlled to an accuracy of better than 0.1 K.

3. Theory

The theory used to analyze the experimental data is the same molecule–surface scattering formalism used to analyze the earlier work on O_2 scattering from graphite [3, 4]. The interaction potential is that of a strongly repulsive wall with a dynamic displacement corrugation due to the motions of the underlying graphite atoms, but having no static corrugation. The theory, which is based on the earlier atom–surface theory of Brako and Newns [10, 11], is in the classical mechanical limit of the transfer of many phonon quanta and includes the correct laws of energy conservation, momentum and angular momentum conservation in the collision.

One way of expressing the fundamental measurable quantities in a molecule–surface scattering experiment is through the differential reflection coefficient (DRC) $dR(\mathbf{p}_f, \mathbf{l}_f; \mathbf{p}_i, \mathbf{l}_i)/d\Omega_f\, dE_f^T$ which gives the fraction of incident molecules with linear momentum $\mathbf{p}_i$ and angular momentum $\mathbf{l}_i$ that are scattered into the state described by $\{\mathbf{p}_f, \mathbf{l}_f\}$ and into a detector that samples the small final solid angle $d\Omega_f$ and small final translational energy dE_f^T. The final translational energy is given by $E_f^T = \mathbf{p}_f^2/2m$ where m is the molecular mass, with a similar expression for the incident translational energy. This differential reflection coefficient is given by [12]

$$\begin{aligned}\frac{dR(\mathbf{p}_f, \mathbf{l}_f; \mathbf{p}_i, \mathbf{l}_i)}{d\Omega_f\, dE_f^T} &\propto \frac{|\mathbf{p}_f|}{p_{iz}} |\tau_{fi}|^2 \left(\frac{\pi}{\Delta E_0^T k_B T_S}\right)\left(\frac{\pi}{\Delta E_0^R k_B T_S}\right)^{1/2} \\ &\times \left(\frac{\pi}{(\Delta E_0^T + \Delta E_0^R) k_B T_S}\right)^{1/2} \exp\left[-\frac{2\mathbf{P}^2 v_R^2}{4\Delta E_0^T k_B T_S}\right] \\ &\times \exp\left[-\frac{2l_z^2 \omega_R^2}{4\Delta E_0^R k_B T_S}\right] \\ &\times \exp\left[-\frac{(E_f^T - E_i^T + E_f^R - E_i^R + \Delta E_0^T + \Delta E_0^R)^2}{4(\Delta E_0^T + \Delta E_0^R) k_B T_S}\right]\end{aligned} \tag{1}$$

where the component of the incident momentum normal to the surface is p_{iz}, the surface temperature is T_S, k_B is the Boltzmann constant, and the recoil energy $\Delta E_0^T = (\mathbf{p}_f - \mathbf{p}_i)^2/2M_S$ is that of a binary collision. The effective target mass is M_S and $\mathbf{P}$ is the component of the total scattering vector $\mathbf{p} = \mathbf{p}_f - \mathbf{p}_i$ parallel to the surface. The final rotational energy of the molecular projectile is denoted by $E_f^R = \mathbf{l}_f^2/2I$ where $\mathbf{l}_f$ is the final angular momentum and I is the classical diatomic molecular moment of inertia, with a similar expression for E_i^R. The total angular momentum transferred in the collision is $\mathbf{l} = \mathbf{l}_f - \mathbf{l}_i$ and l_z is its component normal to the surface. The rotational recoil energy is given by

$$\Delta E_0^R = \frac{l_x^2}{2I_{xx}} + \frac{l_y^2}{2I_{yy}} + \frac{l_z^2}{2I_{zz}}, \tag{2}$$

where the symbols I_{jj} denote the principle components of the effective moment of inertia tensor of the surface. It has been shown by Brako and Newns [10] that the quantity v_R is a weighted average of phonon speeds parallel to the surface and can be completely determined from knowledge of the phonon spectral density, although as is the case here it is usually treated as a constant parameter [10, 13]. A similar role is played by the angular speed constant ω_R for angular momentum transfers, and it can also be computed from knowledge of the dynamical structure function of the surface. The form factor $|\tau_{fi}|^2$ is determined by the interaction force and is the transition matrix of the interaction potential taken between the initial incoming state and the final outgoing state.

An approximate form for $\tau_{\rm fi}$ can be derived from the Born approximation for a typical interaction potential taken in the limit of a hard repulsive wall, a form that has proven useful in describing atom–surface collisions,

$$\tau_{\rm fi} = \frac{2p_{iz}p_{fz}}{m} \tag{3}$$

and this is what is used here [14].

In the present experiments only angular distributions were measured and no information is available on the initial or final rotational state of the projectile molecules. Consequently, in order to compare the measurements to the DRC of equation (1) it must be averaged over incident angular momenta and summed over all possible final angular momenta, leading to a differential reflection coefficient that depends only on linear momenta $\mathrm{d}R\,(\mathbf{p}_{\rm f}, \mathbf{p}_{\rm i})/\mathrm{d}\Omega_{\rm f}\,\mathrm{d}E_{\rm f}^{\rm T}$. To obtain an angular distribution this differential reflection coefficient must be integrated over all final translational energies, taking into account the energy efficiency of the detector. For the present experiments, the detector is a density detector in which the detection efficiency decreases in inverse proportion to the final translational speed. Taking into account that for a fixed source–detector experiment the final angle $\theta_{\rm f}$ depends on the incident angle $\theta_{\rm i}$ through the relation $\theta_{\rm f} + \theta_{\rm i} = \theta_{\rm SD}$, the in-plane angular distributions discussed in section 4 below can be written as functions of $\theta_{\rm f}$ given by

$$\frac{\mathrm{d}R(\theta_{\rm f})}{\mathrm{d}\Omega_{\rm f}} = \int_0^\infty \frac{1}{\sqrt{E_{\rm f}^{\rm T}}} \frac{\mathrm{d}R}{\mathrm{d}\Omega_{\rm f}\,\mathrm{d}E_{\rm f}^{\rm T}}\,\mathrm{d}E_{\rm f}^{\rm T}. \tag{4}$$

There are several parameters that remain fixed for the calculations used to analyze the data and these were chosen as follows. For all calculations $v_{\rm R}$ was chosen to be 3000 m s^{-1} and $\omega_{\rm R}$ was chosen to be 1×10^{10} s^{-1}. The value of $\omega_{\rm R}$ is so small that changes in its value of even up to an order of magnitude have only a negligible effect on the calculations. The incident rotational temperature of the molecular beam is not known, so both molecular species were given an initial rotational energy of 2.6 meV corresponding to a rotational temperature of about 30 K. This is consistent with the knowledge that molecular jet beams typically have a cold rotational temperature. The effective surface moment of inertia may be expected, in the case of a molecular target, to be that of a surface molecule. However, there can be collective effects especially in the case of large projectiles that can strike more than one surface molecule simultaneously, and in that case it is expected to become larger than that of a single surface molecule. For this study a value of $I_{jj} = 3.99 \times 10^{-46}$ kg m^2 was taken. This is approximately the moment of inertia of a single six-atom carbon ring calculated with respect to an axis through the plane of the ring. Again, there is not a strong dependence of the calculated results on the choice of the effective moment of inertia. The value of the molecular projectile moment of inertia I was calculated using the known masses and molecular dimensions which gives $I = 1.40 \times 10^{-46}$ kg m^2 for N_2 and $I = 1.46 \times 10^{-46}$ kg m^2 for CO.

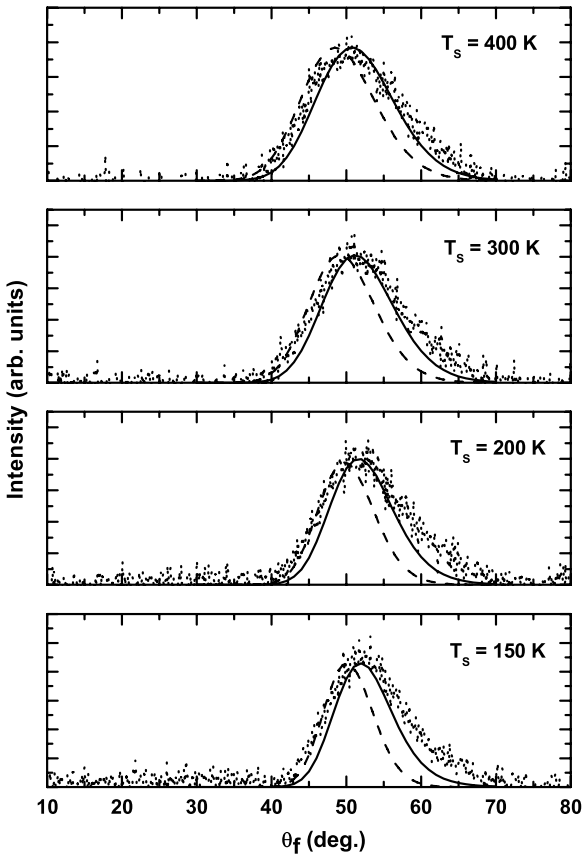

Figure 1. Angular distribution intensity spectra, shown as a function of final scattering angle $\theta_{\rm f}$, for scattering of CO from graphite taken with a fixed source–detector angle $\theta_{\rm SD} = 90°$ and for incident translational energy $E_{\rm i}^{\rm T} = 277$ meV. The surface temperature $T_{\rm S}$ ranges from 150 to 400 K as marked. The points are the measured experimental data, the solid curves are the rigid diatomic calculations and the dotted curves are the pseudo-atomic calculations, all with an effective surface mass equal to 1.8 benzene rings of carbon.

4. Results

4.1. CO scattering from graphite

A collection of four angular distribution intensity spectra for a CO molecular beam scattering from a graphite surface is shown as a function of $\theta_{\rm f}$ in figure 1. The data were taken at the fixed incident translational energy of 277 with surface temperatures ranging from 150 to 400 K.

The data are compared with the rigid diatomic calculations derived from the DRC of equation (1) as shown in the solid curves. The value for the effective surface mass $M_{\rm S}$ was chosen largely by matching the most probable final angles of the calculations to those of the experimental data at all temperatures and incident energies at which measurements were made. The results are sensitive to the choice of $M_{\rm S}$, and the calculations show that increasing $M_{\rm S}$ by that of a single six-atom carbon ring will shift the most probable angle by as much as 2°. This process resulted in an estimate of the effective surface mass of approximately that of 1.8 benzene rings of carbon (10.8 carbon atoms, or 129.6 amu). This value

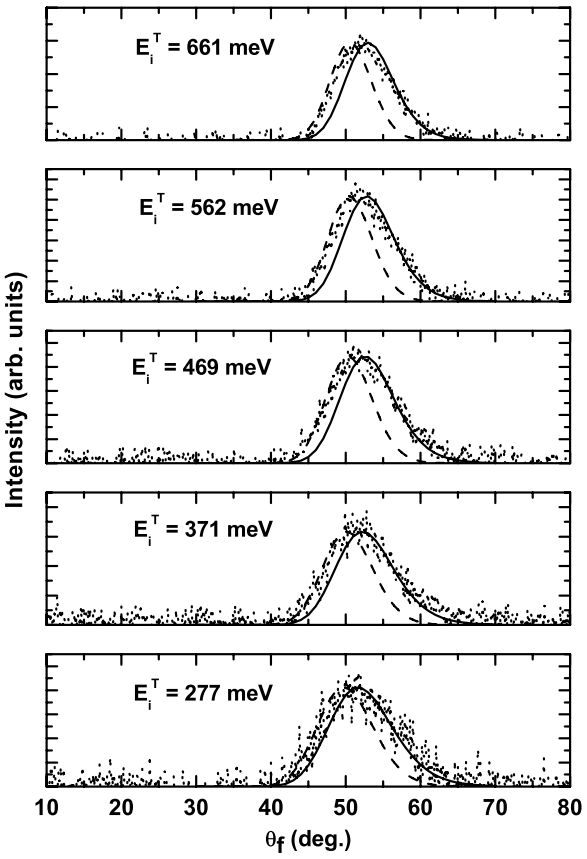

Figure 2. Angular distribution intensity spectra similar to figure 1 except for a fixed surface temperature $T_S = 200$ K and incident translational energies ranging from 277 meV to 661 meV as marked.

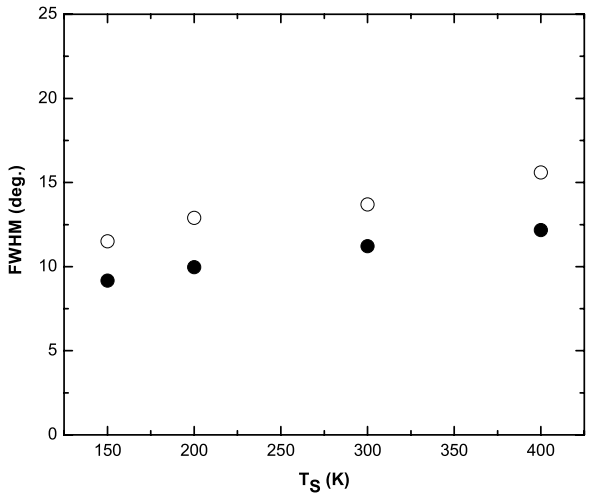

Figure 3. Full width at half maximum (FWHM) as a function of surface temperature T_S. The incident translational energy is 277 meV. The open circles are CO data and the filled circles are rigid molecular theory calculations.

is the same as found earlier for the case of O_2 scattering from graphite [3, 4]. A value of approximately 1.8 carbon benzene rings is also what is found for N_2 scattering as discussed in section 4.3 below. This collective effect implied by the need for a larger surface effective mass has been recognized previously in atom–surface collisions for Xe scattering [7, 8] and for Ar scattering [15] from graphite. It appears that the very strong in-plane bonding of the carbon atoms in the outermost graphene plane causes a large number of C atoms to respond nearly simultaneously to the collision of the molecular projectile.

For comparison, shown also in figure 1 as dashed curves are pseudo-atomic calculations using the smooth surface scattering model for atomic projectiles [17]. In these calculations the projectile is taken to be an atomic particle with the same mass as CO, and the effective surface mass is kept the same. These pseudo-atomic calculations at all temperatures and incident energies tend to peak at an angle several degrees closer to the specular position than those of the corresponding diatomic CO projectile. Both sets of calculated curves, however, have the same general temperature and incident energy dependence as the data and strongly indicate that the collision process is a single scattering event with a collective surface.

The data for the angular distributions as a function of incident translational energy are shown in the series of five spectra in figure 2. All of these spectra were taken at a surface temperature of 200 K and the incident kinetic energy ranges from 277 to 661 meV. As in figure 1 the solid curves show the calculations carried out with the molecular differential reflection coefficient of equation (1) and the dashed curves show the results of the simpler pseudo-atomic scattering model. The pseudo-atomic curves are, as before, shifted somewhat towards the specular position.

Although figures 1 and 2 illustrate the nature of the observed angular distributions and are reasonably well interpreted by the molecular scattering theory embodied in equation (1) it is of interest to examine more closely the details of this description. This is done in figures 3–8 which illustrate in more detail the behavior of the observed angular distributions on both surface temperature and incident translational energy.

Figure 3 gives the temperature dependence of the full width at half maximum (FWHM) of the angular distributions. The open circles show the experimental data taken from figure 1 at the fixed incident energy of 277 meV. The data indicate that the FWHM increases monotonically by about 4° over the temperature range from 150 to 400 K. The results of the calculations of the molecular scattering theory are shown as filled circles. The calculations have the same increasing trend with temperature and nearly the same slope as the experimental points, but the calculated FWHM is about 3° smaller than the experiment at all points. The increasing FWHM with temperature is consistent with the behavior exhibited in the energy-resolved differential reflection coefficient intensity of equation (1), which indicates that the temperature dependence of the DRC width is primarily driven by that of the argument of the Gaussian-like factor, i.e. an approximate temperature dependence that goes as $\sqrt{T_S}$. Although the angular distributions are summed over rotational energies and final translational energy, figure 3 shows that this increasing behavior persists even after these sums are taken.

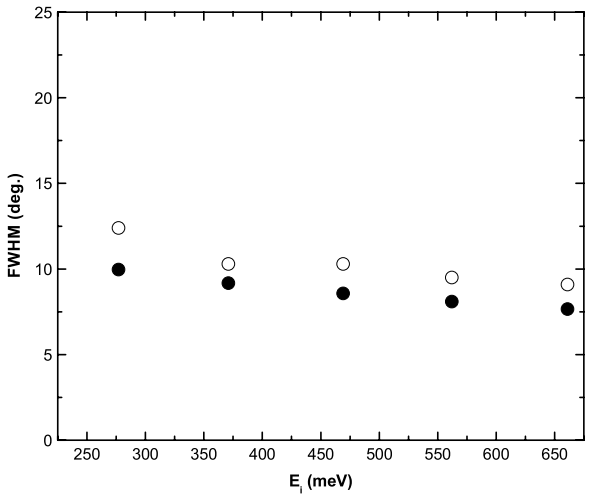

Figure 4. Full width at half maximum (FWHM) as a function of incident translational energy E_i^T at the fixed surface temperature of 200 K. The open circles are CO data and the filled circles are rigid molecular theory calculations.

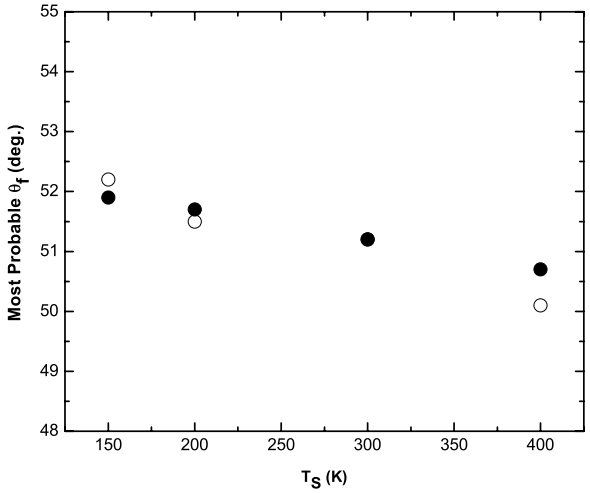

Figure 5. Most probable final angular position as a function of temperature for a fixed incident translational energy of 277 meV. Experimental points for CO are open circles and calculations with the rigid molecular theory are filled circles.

The FWHM is again exhibited in figure 4, this time as a function of incident translational energy. The experimental data shown as open circles are taken from figure 2 and the surface temperature is 200 K. As opposed to the case of the temperature dependence of figure 3, the FWHM decreases slightly with incident energy, with a total decrease of about 3° as the energy ranges from 277 to 661 meV. The experimental point at $E_i^T = 277$ meV in figure 4 shows a slightly smaller FWHM than the corresponding point in figure 3. This is because the two sets of angular distribution data in figures 1 and 2 were taken at different times.

The fact that the FWHM decreases as a function of incident translational energy is not immediately predictable from the behavior of the energy-resolved differential reflection coefficient of equation (1). In fact, the state-to-state differential reflection coefficient of equation (1) has a Gaussian-like factor that increases with incident translational

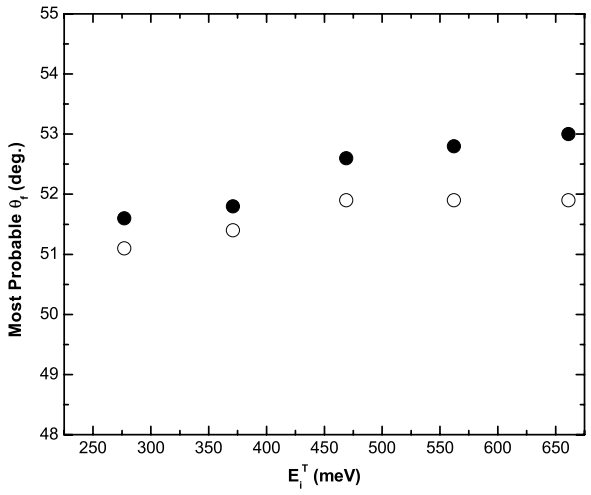

Figure 6. Most probable final angular position as a function of incident translational energy. The temperature is 200 K, experimental points for CO are open circles and calculations are filled circles.

energy. This is evident from the argument of the Gaussian-like factor, in which the width of the peak is governed by the product of $\Delta E_0^T T_S$, i.e. when conditions are such that the shape of the peak is approximately Gaussian then the FWHM will increase as $\sqrt{\Delta E_0^T T_S}$. Under the same conditions in which the peak appears approximately Gaussian in shape, then the recoil energy ΔE_0^T is nearly proportional to E_i^T, implying that the width of the energy-resolved intensity should increase as $\sqrt{E_i^T}$, i.e. the width of the DRC has a similar dependence for both temperature and incident translational energy. It is not immediately evident that this increasing behavior should persist in the angular distributions, which are obtained after summing the differential reflection coefficient over final translational energies and rotational momenta. However, the calculations show a small but clear decreasing behavior of the angular distribution FWHMs with increasing incident translational energy, which is in agreement with the experiment.

The measured FWHMs of figures 3 and 4 are consistently larger than those predicted by the calculations by a roughly constant value at all points measured. This difference may be ascribed to other scattering mechanisms, not included in the theory and that do not depend strongly on temperature or incident translational energy. Scattering from defects on the graphite surface has been proposed as a possible mechanism [3, 15, 16].

Figures 5 and 6, respectively, show the most probable final angle (or peak position) of the angular distributions as a function of temperature and incident translational energy. The most probable final angle is seen to be remarkably stable as a function of T_S or E_i^T over the entire measured range of both of these experimentally controllable variables and the calculations support this observation. As mentioned above, the small difference noted in the corresponding experimental values at energy 277 meV and temperature 200 K in figures 5 and 6 is due to the fact that they are derived from data sets taken at different times.

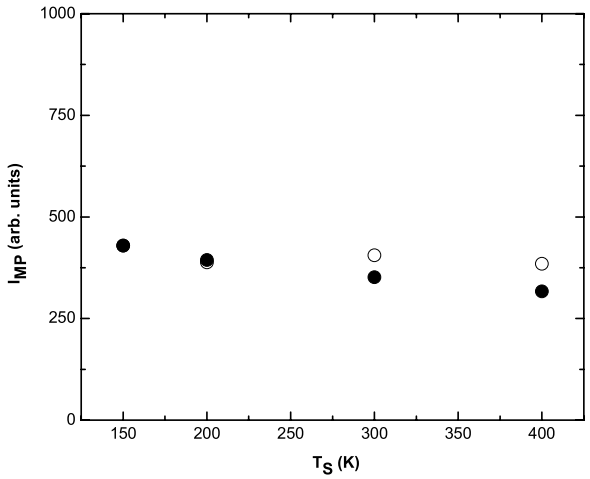

Figure 7. Most probable final intensity as a function of surface temperature T_S for an incident translational energy of 277 meV. The data for CO are shown as open circles. Rigid molecular theory calculations are shown as filled circles. The experimental point at the lowest temperature is normalized to the calculation.

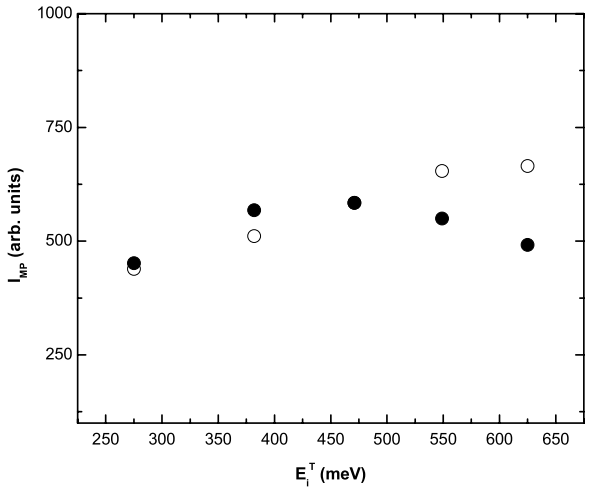

Figure 8. Most probable final intensity as a function of incident translational energy with $T_S = 200$ K. The data points for CO, corrected for incident flux intensity, are shown as open circles. Rigid molecular theory calculations are shown as filled circles. The experimental point is normalized to coincide with the calculated point at $E_i^T = 469$ meV.

Figures 7 and 8 give, respectively, the T_S and E_i^T dependence of the angular distribution peak intensities (most probable intensities). As a function of temperature in figure 7 the calculations show a decreasing behavior in the maximum intensity. Such decreasing behavior is exhibited in the differential reflection coefficient of equation (1) by the products of inverse powers of T_S in its prefactors. It is interesting that such decreasing behavior persists in the angular distributions. This decrease is also apparent in the experimentally measured values, but to a lesser degree at larger temperatures.

Measurement of accurate relative intensities for varying incident translational energies presents a problem that goes well beyond those that exist when simply changing simpler

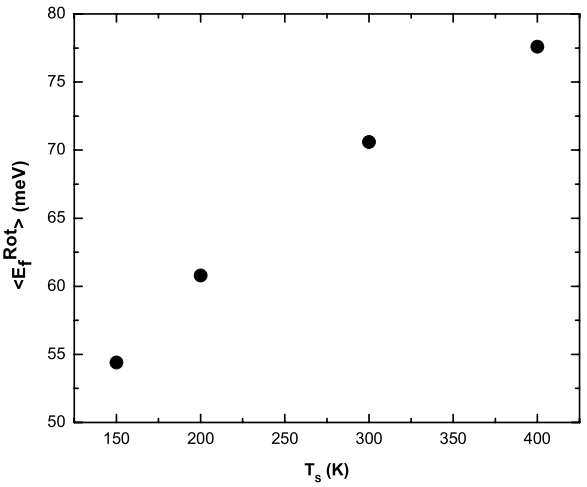

Figure 9. CO/graphite: calculated final rotational energy as a function of surface temperature. The incident translational energy is 277 meV with surface temperatures and most probable final angles corresponding to those of figure 1.

experimental parameters such as the temperature of the target sample while leaving the characteristics of the incident beam unchanged. In order to increase the incident beam energy, either the temperature of the beam stagnation chamber is raised or the ratio of the seeding rare gas is changed as is done here. In either case this affects the incident flux, and in addition at each incident energy one adjusts the stagnation chamber pressure in order to maximize the energy resolution. Consequently, at each new beam energy a correction must be made to account for the change in incident intensity. An accepted way of accomplishing this is to apply a correction factor to the incident flux according to the relative pressures in the sample chamber when the incident beam is turned on and when it is turned off. The correction factor at each incident energy is the ratio of relative pressure in the sample chamber divided by the pressure when the beam is turned off. In figure 8 all data have been corrected in this manner. The data in figure 8 exhibit a monotonically increasing dependence on incident translational energy. The calculations initially show increasing behavior at lower temperatures, but then begin to decrease at energies above 500 meV.

4.2. Calculations of rotational and translational energy transfers in CO scattering

It is of interest to give estimates of expected rotational and translational energy transfers to or from the molecule during the collision process. Although energy-resolved measurements were not carried out in this study, the reasonable agreement with data for the measured angular distributions obtained through calculations with the molecular scattering differential reflection coefficient of equation (1) lend some confidence to the predictions of this model for energy transfers.

Figure 9 shows calculations of the average final rotational energy of the CO molecules as a function of surface temperature after scattering. In all cases the incident

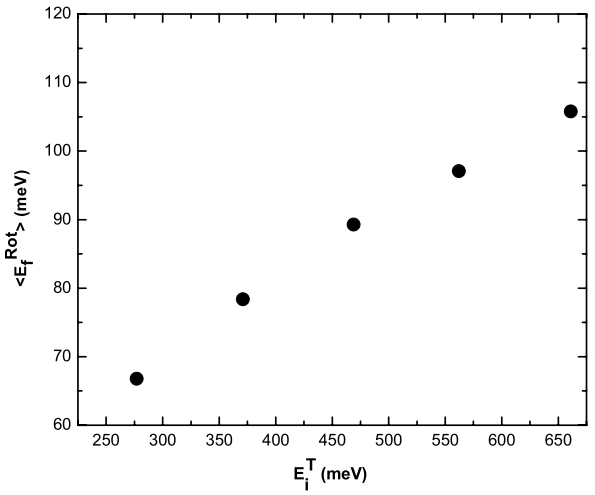

Figure 10. CO/graphite: calculated final rotational energy as a function of incident energy. The surface temperature is $T_S = 200$ K with incident energies and most probable final angles corresponding to those of figure 2.

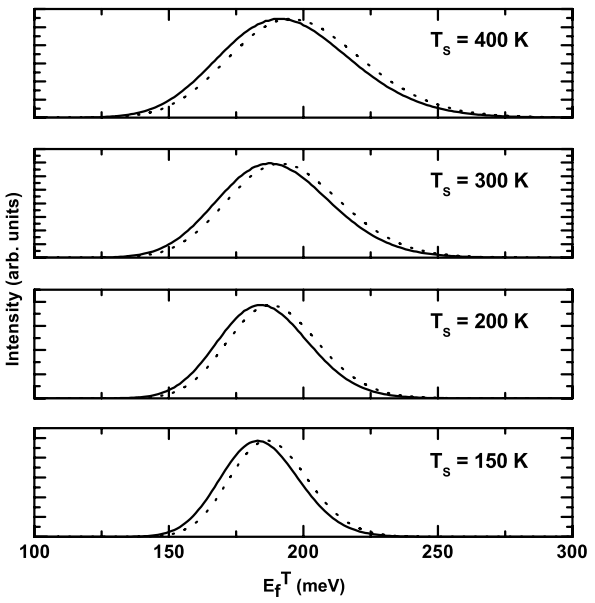

Figure 11. CO/graphite: solid curves—rigid molecular theory differential reflection coefficient as a function of final translational energy for all temperatures shown in figure 1 as marked, evaluated at the most probable final angle of the angular distribution spectrum for each temperature. The incident translational energy is 277 meV. The dotted curves show the pseudo-atomic calculation evaluated at the same conditions and for the same effective mass of 1.8 carbon rings.

translational energy is 277 meV and the final angle at each temperature is the most probable angle, or in other words all other incident conditions are taken at the most probable (or largest) intensity of figure 1. These initial conditions were chosen in order to predict the rotational energy transfer expected at the point of largest intensity in the final angular distribution spectra. It is seen from figure 9 that the predicted rotational energy transfers to the molecule are large and increase significantly, although not linearly, with temperature.

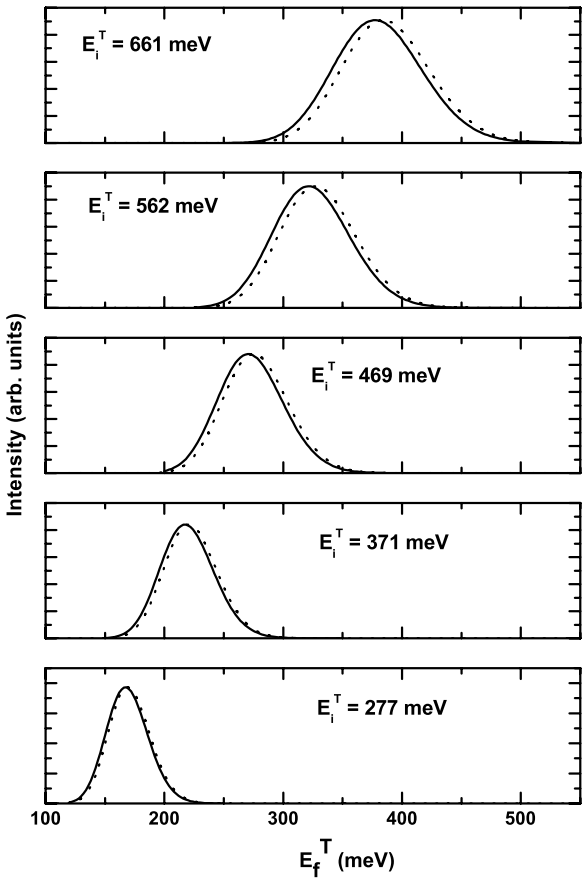

Figure 12. CO/graphite: solid curves—rigid molecular theory differential reflection coefficient as a function of final translational energy for all incident translational energies shown in figure 2 as marked, evaluated at the most probable final angle of the angular distribution spectrum for each incident energy. The surface temperature is 200 K. The dotted curves show the pseudo-atomic calculation evaluated at the same final translational conditions and for the same effective mass of 1.8 carbon rings.

The calculated average final rotational energies range from about 55 meV at the lowest temperature of 150 K, already significantly larger than the incident rotational energy of 2.6 meV, to nearly 80 meV at the highest temperature of 400 K.

Figure 10 shows results of similar calculations for the average final rotational energy as a function of incident translational energy. The initial conditions for each point calculated correspond to the point of maximum intensity (the most probable intensity) in each of the corresponding panels of figure 2. Again, the rotational energy transfers are large and final values range from over 60 meV at the lowest incident translational energy of 277 meV to more than 100 meV at the highest translational energy of 661 meV. The monotonic dependence on incident translational energy is nearly linear, but slightly less strong than linear.

Figures 11 and 12 give calculations that show expected translational energy losses to the surface as functions of temperature and incident translational energy. What is shown in figure 11 are the differential reflection coefficients of equation (1), summed over all final rotational energies,

evaluated as a function of final translational energy for initial conditions corresponding to the most probable intensity of each panel of figure 1. The incident energy is 277 meV and this basically illustrates the temperature dependence of the manner in which translational energy is transferred to the surface as heat. The most probable final translational energy is about 180 meV, implying a prediction for the energy loss to the surface of about 100 meV. The FWHM of the energy transfer spectrum increases with temperature approximately according to the expected $\sqrt{T_S}$ behavior. Also shown in each panel of figure 11 as a dashed curve is the pseudo-atomic calculation evaluated under the same conditions. The two curves are quite similar in appearance, but the pseudo-atomic curve exhibits slightly less translational energy loss. The difference between the molecular and the pseudo-atomic curves is an indicator of the additional incident translational energy that is converted to molecular rotational energy in the collision, as compared to the collision of a similar atomic-like projectile.

Figure 12 shows a similar calculation giving the predicted dependence on initial translational energy of the energy-resolved differential reflection coefficient. Shown as the solid curves are the results of equation (1), after summing over all final rotational energies, with initial conditions corresponding to the most probable intensity positions of each of the five panels of figure 2. The lower panel of figure 12 is the same as the 200 K panel of figure 11. Two aspects are immediately apparent, final translational energy-resolved spectra are predicted to have FWHMs that increase nearly as the square root of E_i^T, as discussed above in connection with figure 4, and the energy transferred to the surface increases substantially and nearly linearly with incident translational energy. It is seen that for the lowest incident energy of 277 meV the predicted energy loss is about 100 meV, while for the highest energy of 661 meV the translational energy transferred to the surface is over 250 meV. The dashed curves show the results of the pseudo-atomic calculation, with all other initial experimental parameters held the same. As exhibited above in figure 11 the pseudo-atomic calculation predicts somewhat less translational energy loss, and the difference between the two curves is explained as the effect of transferring translational into rotational energy in the case of the molecular projectile.

4.3. N_2 scattering from graphite

The above section 4.1 gives a discussion of the experimental observations and measurements of angular distributions for the scattering of CO from the graphite surface. This section describes a similar set of angular distribution measurements for the diatomic molecule N_2 scattered from graphite. Figure 13 shows the data for six different angular distributions all taken with an incident translational energy of 275 meV but having surface temperatures ranging from 150 to 400 K. The solid curves show the calculated results for the angular distribution intensities based on the differential reflection coefficient of equation (1), while the dashed curves show the corresponding pseudo-atomic calculation for an atomic

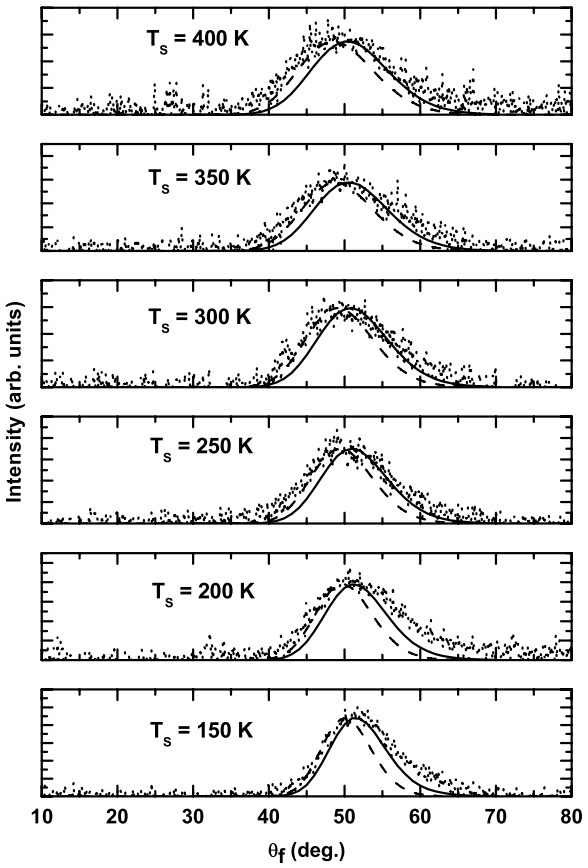

Figure 13. Similar to figure figure 1 except for N_2 scattering from graphite: angular distribution intensity spectra for incident translational energy $E_i^T = 275$ meV. The surface temperature T_S ranges from 150 to 400 K as marked. The solid curves are the rigid diatomic calculations and the dashed curves are the pseudo-atomic calculations, all with an effective surface mass equal to 1.8 carbon rings.

projectile with the same mass as N_2. Figure 14 shows five angular distributions all for the same temperature of 200 K, but with incident translational energies ranging from 275 to 625 meV. The theoretical calculations shown as solid and dashed curves are the same as in figure 13. As mentioned above, the calculations were carried out with an effective surface mass of 1.8 carbon rings.

The details of the characteristic widths, positions and intensities of these angular distributions are discussed in figures 15 through 20 in a manner similar to the discussion for the CO data above. The FWHMs are shown as open circular points in figures 15 and 16, where it is seen that as a function of temperature the observed widths increase while as a function of incident translational energy they decrease slightly. In both cases, the calculations based on the classical molecular scattering model and shown as the filled circles reproduce these behavior trends in temperature and energy, but are consistently smaller than the measured values. Again, this implies the presence of additional temperature and energy independent mechanisms present which are not included in the theory, such as the possibility of scattering by defects or other impurities or imperfections on the surface.

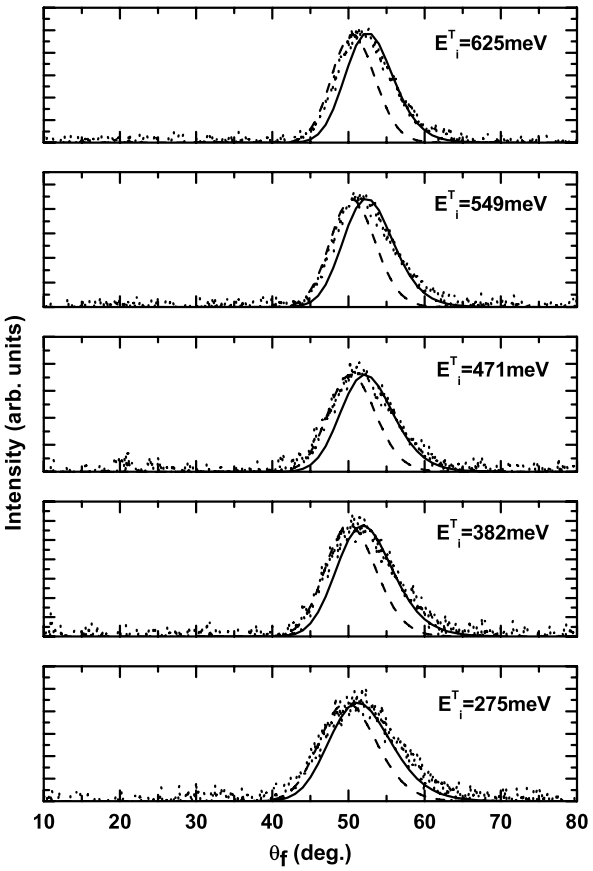

Figure 14. Angular distribution intensity spectra similar to figure 13 except for a fixed surface temperature $T_S = 200$ K and incident translational energies ranging from 275 meV to 625 meV as marked.

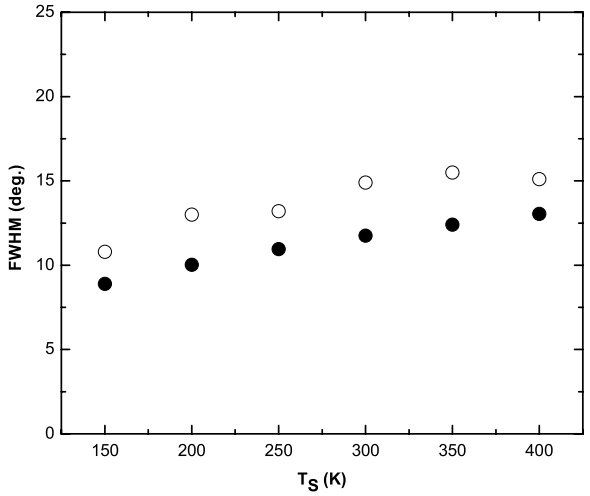

Figure 15. N_2 scattering from graphite: FWHM as a function of surface temperature T_S. The incident translational energy is 275 meV. The open circles are N_2 data and the filled circles are rigid molecular theory calculations.

The most probable final angular positions are shown in figures 17 and 18 as functions of temperature and translational energy, respectively. These peak positions show very little change as the temperature or energy are increased.

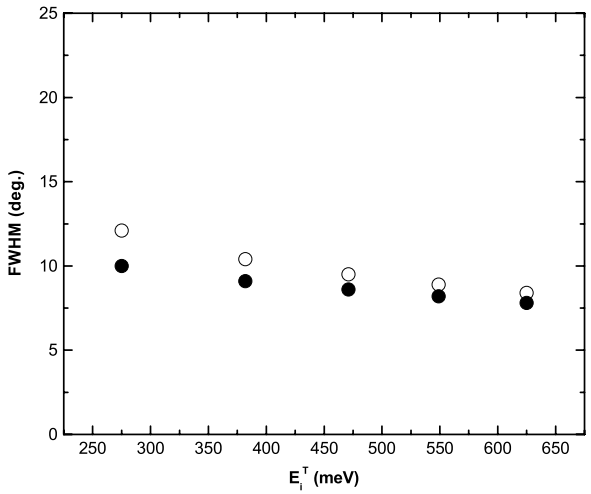

Figure 16. N_2 scattering from graphite: FWHM as a function of incident translational energy E_i^T at the fixed surface temperature of 200 K. The open circles are data and the filled circles are rigid molecular theory calculations.

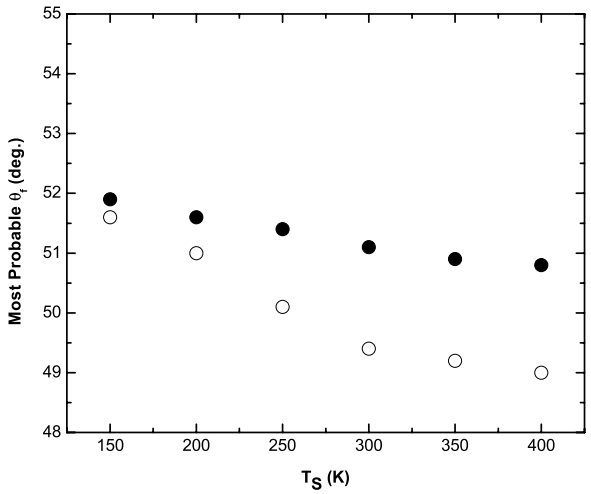

Figure 17. N_2 scattering from graphite: most probable final angular position as a function of temperature for a fixed incident translational energy of 275 meV. Experimental points are open circles and calculations with the rigid molecular theory are filled circles.

Again, the calculations based on the molecular scattering model are shown as solid circles and agree well with the observed behavior. The small discrepancy in position of the experimental points at the common temperature of 200 K and incident energy of 275 meV is due to the fact that the data were taken at two different times.

Figures 19 and 20 show as open circular points the temperature and energy dependence of the measured most probable intensities of the angular distributions. As a function of temperature the most probable intensity decreases, as expected, based on arguments involving overall unitarity of the scattering process. This observed decrease is reproduced reasonably well by the calculations, shown also in figure 19 as filled circles. As a function of increasing incident translational energy, the most probable intensity is observed to be a

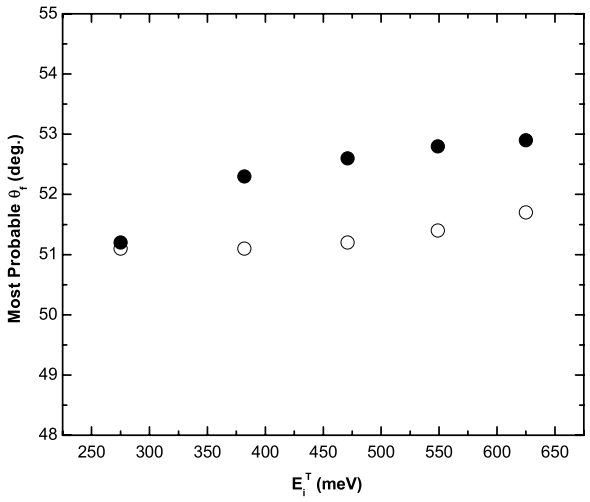

Figure 18. N_2 scattering from graphite: most probable final angular position as a function of incident translational energy. The temperature is 200 K, experimental points are open circles and calculations are filled circles.

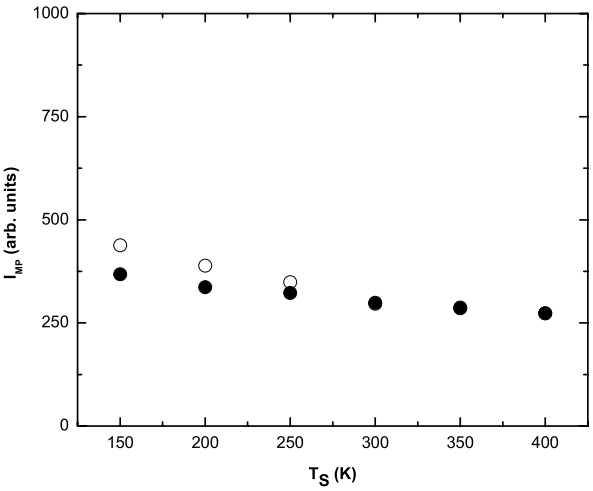

Figure 19. N_2 scattering from graphite: most probable final intensity as a function of surface temperature T_S for an incident translational energy of 275 meV. The data are shown as open circles. Rigid molecular theory calculations are shown as filled circles. At the three highest temperatures the data and calculational points coincide.

monotonically increasing quantity, as shown in the open circle points in figure 20. The calculations show initial increasing behavior at lower energies, but then give decreasing values of the most probable intensity at the larger temperatures above 500 K similar to the behavior of CO and also that observed earlier of O_2 scattering from graphite [3].

5. Discussion and conclusions

In this paper we have presented new data for the scattering of carbon monoxide and nitrogen molecules from a clean and ordered graphite surface. For well-defined incident molecular beams, scattered angular distribution spectra are presented for surface temperatures ranging from 150 to 400 K and for

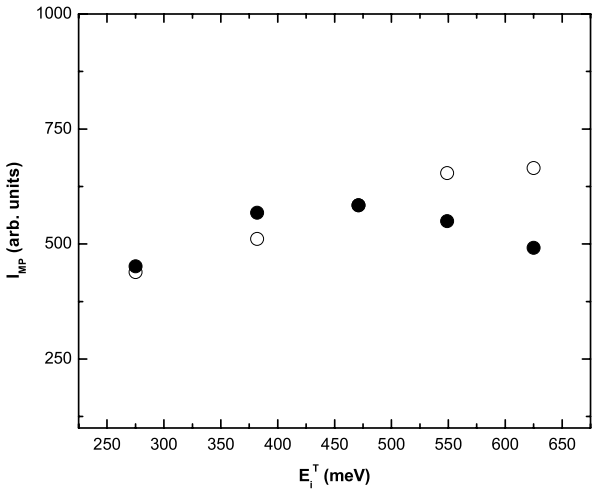

Figure 20. N_2 scattering from graphite: most probable final intensity as a function of incident translational energy with $T_S = 200$ K. The data points, corrected for incident flux intensity, are shown as open circles. Rigid molecular theory calculations are shown as filled circles. At the point with incident translational energy of 471 meV the experimental point is normalized to coincide with the calculated point.

incident translational energies from 275 to over 650 meV. These angular distributions appear as single-peaked structures whose most probable intensities are located at somewhat supraspecular angles that are not strongly dependent on temperature or incident translational energy. The widths and relative intensities are, though, quite dependent on temperature and energy.

However, it is interesting to note that no clear signature of distinguishing differences was observed between the scattering of CO and that of N_2 from the graphite surface, and it is of interest to discuss this. Both molecules have almost the same molecular mass, but their molecular structure and electric dipole moments are different. Thus the scattering events are expected to be different. Indeed, the scatterings of CO and N_2 molecules are reported to be quite different in the cases from Ag(111) [18–20], Ni(111) [21, 22], and LiF(001) [9, 23]. However, from the graphite surface, both molecules show very similar angular intensity scattering distributions under all measured experimental conditions as shown in figures 1–8 and 13–20, respectively. This suggests that both effects of the molecular structure and electronic dipole are not significant for the scattering event in the case of the graphite surface. It appears that, contrary to the case of metallic surfaces or even the insulator LiF(001), the scattering of these molecules from graphite is predominantly mechanical. This is possibly due to the large cooperative motion of light carbon atoms at the scattering event in the case of flat graphite, as represented by the large effective mass derived from the analysis by the theoretical calculation. That is to say, large cooperative motion may result in a 'trampoline'-like motion [8] of the graphite layers, leading to a smearing effect on the molecular structure difference and electronic dipole difference in the scattering events between CO and N_2.

These data are analyzed in terms of a molecular scattering model based on classical mechanics. This model was also used to analyze earlier angular distribution data for the scattering of O_2 molecules from graphite. It assumes an interaction potential of a hard repulsive surface with no static corrugation, but with a dynamic thermal corrugation due to the vibrations of the underlying atoms near the surface. Only single-collision processes with the surface are considered. Correct conservation of energy, linear momentum and angular momentum are included for both translational and rotational degrees of freedom of the molecular projectiles.

Good agreement between the data and calculations with the molecular scattering model are obtained for the dependence of the angular distributions on both temperature and incident translational energy. However, this agreement is obtained only upon assuming that the effective mass of the surface in the single-collision event is significantly larger than that of a single carbon atom. We find the effective surface mass is 1.8 rings of six-atom carbon (10.8 carbon atoms) for both CO and N_2 scattering, the same as in previous work for O_2 scattering from graphite [3]. Similarly large values of the effective mass have been obtained from earlier scattering experiments using the heavy rare gases Ar and Xe scattering from graphite [7, 8, 15]. In addition to the direct comparisons of the theoretical model with the available data, additional calculations were presented for eventual comparison with experiments having the capability of resolving the final translational and rotational energy of the scattered spectra. These calculations indicate that the scattered molecules, under typical conditions near the most probable intensities of the observed angular distributions, leave the surface with greatly enhanced rotational energy but significantly less translational energy.

Based on the observed characteristics of the angular distribution spectra and the agreement found with the single-collision molecular scattering model, it is concluded that the predominant scattering mechanism is a single collision with a collective surface involving several carbon atoms. This is the same conclusion that was arrived at for the case of O_2 scattering and for Ar and Xe scattering from graphite. It is likely that most of the collective carbon atoms are in the outermost graphene layer because of the extremely strong in-plane bonding of the carbon atoms, as opposed to the weak Van der Waals forces between graphene layers below the surface. The strength of this outer graphene layer and the role it plays in the single-collision reflection of the projectiles is the reason the scattering has been termed a 'trampoline' effect [8].

The experiments reported here, together with the earlier work with oxygen molecules [3], provide useful information and an important data base for illuminating the characteristic behaviors of small molecular projectiles interacting with graphite surfaces with incident energies in the eV range. The success of the theoretical model in explaining the observed angular distributions lends some confidence in its ability to predict the behavior of the scattered spectra with respect to experimentally controllable parameters other than the temperature and energy investigated here, such as variations of incident or detector angles or measurements with final translational or rotational energy and momentum resolution.

Acknowledgments

The authors would like to acknowledge financial support from the Japanese Ministry of Education, Culture, Sports, Science and Technology (MEXT), under the Grant-in-Aid for Young Scientists (B) 23760024 of Japan.

References

[1] Hasselbrink E and Lundqvist B (ed) 2008 *Surface Dynamics* (*Handbook of Surface Science* vol 3) (Amsterdam: Elsevier)
[2] Barker J A and Auerbach D J 1985 *Faraday Discuss.* **80** 277
[3] Oh J, Kondo T, Arakawa K, Saito Y, Hayes W W, Manson J R and Nakamura J 2011 *J. Phys. Chem.* A **115** 7089
[4] Hayes W W, Oh J, Kondo T, Arakawa K, Saito Y, Nakamura J and Manson J R 2012 *J. Phys.: Condens. Matter* **24** 104010
[5] Ambaye H and Manson J R 2006 *J. Chem. Phys.* **125** 084717
[6] Hayes W W and Manson J R 2011 *J. Phys. Chem.* A **115** 6838
[7] Watanabe Y, Yamaguchi H, Hashinokuchi M, Sawabe K, Maruyama S, Matsumoto Y and Shobatake K 2005 *Chem. Phys. Lett.* **413** 331
[8] Watanabe Y, Yamaguchi H, Hashinokuchi M, Sawabe K, Maruyama S, Matsumoto Y and Shobatake K 2006 *Eur. Phys. J.* D **38** 103
[9] Kondo T, Kato H S, Yamada T, Yamamoto S and Kawai M 2006 *Eur. Phys. J.* D **38** 129
[10] Brako R and Newns D M 1982 *Phys. Rev. Lett.* **48** 1859
[11] Brako R and Newns D M 1982 *Surf. Sci.* **117** 422
[12] Ambaye H, Manson J R, Weibe O, Wesenberg C, Binetti M and Hasselbrink E 2004 *J. Chem. Phys.* **121** 1901
[13] Meyer H-D and Levine R D 1984 *Chem. Phys.* **85** 189
[14] Goodman F O and Wachman H Y 1976 *Dynamics of Gas-surface Scattering* (New York: Academic)
[15] Yamada Y, Sugawara C, Satake Y, Yokoyama Y, Okada R, Nakayama T, Sasaki M, Kondo T, Oh J, Nakamura J and Hayes W W 2010 *J. Phys.: Condens. Matter* **22** 304010
[16] Oh J, Kondo T, Hatake D, Honma Y, Arakawa K, Machida T and Nakamura J 2010 *J. Phys.: Condens. Matter* **22** 304008
[17] Hayes W W and Manson J R 2007 *J. Chem. Phys.* **127** 164714
[18] Kummel A C, Sitz G O, Zare R N and Tully J C 1988 *J. Chem. Phys.* **89** 6947
[19] Hanisco T F, Yan C and Kummel A C 1993 *J. Vac. Sci. Technol.* A **11** 2090
[20] Leatherman G S and Diehl R D 1997 *Langmuir* **13** 7063
[21] Hines M A and Zare R N 1993 *J. Chem. Phys.* **98** 9134
[22] Matthews C M, Balzer F, Hallock A J, Ellison M D and Zare R N 2000 *Surf. Sci.* **460** 12
[23] Kondo T, Kato H S, Yamada T, Yamamoto S and Kawai M 2005 *J. Chem. Phys.* **122** 244713